J. Biochem. 127, 345–350 (2000)

Functional Analysis of Conserved Aspartate and Histidine Residues Located Around the Type 2 Copper Site of Copper-Containing Nitrite Reductase[1]

Kunishige Kataoka,[2] Hiroshi Furusawa, Kohichi Takagi, Kazuya Yamaguchi, and Shinnichiro Suzuki

Department of Chemistry, Graduate School of Science, Osaka University, 1-16 Machikaneyama, Toyonaka, Osaka 560-0043

Received September 20, 1999; accepted December 9, 1999

A heterologous expression system of the blue copper–containing nitrite reductase from *Alcaligenes xylosoxidans* GIFU1051 (*Axg*NIR) was constructed, and the purified recombinant enzyme was characterized. All the characteristic spectroscopic properties and enzyme activity of native *Axg*NIR were retained in the copper-reconstituted recombinant protein expressed in *Escherichia coli*, indicating the correct coordination of two types of Cu (type 1 and 2) in the recombinant enzyme. Moreover, two conserved noncoordinate residues, Asp98 and His255, located near the type 2 Cu site were replaced to elucidate the catalytic residue(s) of NIR. The Asp98 residue hydrogen-bonded to the water molecule ligating the type 2 Cu was changed to Ala, Asn, or Glu, and the His255 residue hydrogen-bonded to Asp98 through the water molecule was replaced with Ala, Lys, or Arg. The catalytic rate constants of all mutants were decreased to 0.4–2% of those of the recombinant enzyme, and the apparent K_m values for nitrite were greatly increased in the Asp98 mutants. All the steady-state kinetic data of the mutants clearly demonstrate that both Asp98 and His255 are involved not only in the catalytic reaction but also in the substrate anchoring.

Key words: *Alcaligenes xylosoxidans*, copper protein, nitrite reductase, type 1 Cu, type 2 Cu.

Nitrite reductase (NIR) is a key enzyme in the alternative respiration system of the denitrifying bacteria (*1*). In the denitrifying pathway ($NO_3^- \rightarrow NO_2^- \rightarrow NO \rightarrow N_2O \rightarrow N_2$), NIR accepts one electron from an electron donor and catalyzes the reduction of NO_2^- to NO. Two types of NIR containing Cu or hemes *c* and d_1 have so far been reported (*1, 2*). Copper-containing nitrite reductase (NIR) has two Cu centers, one each of type 1 Cu (blue copper) and type 2 Cu (nonblue copper), per monomer [M_r = *ca.* 36,000 (*3*)]. Type 1 Cu accepts an electron from an external electron carrier, resulting in blue (*4*) or green (*5, 6*) coloration. Type 2 Cu which accepts an electron from the reduced type 1 Cu site, is the reduction center of NO_2^- (*7*).

Cloning and expression of three green NIRs from *Achromobacter cycloclastes* IAM 1013 [*Aci* (*8*)], *Alcaligenes faecalis* S-6 [*Afs* (*9*)], and *Rhodobacter sphaeroides* 2.4.3 [*Rhs* (*10*)] have been reported. Recently, two *Alcaligenes* blue NIR genes of *A. xylosoxidans* NCIMB 11015 (*Axn*) and *A. xylosoxidans* GIFU1051 [*Axg* (*11*)] have been cloned independently by Kohzuma *et al.* (*12*) and our group[3], respectively. The expression system of *Axn*NIR was reported by Prudencio *et al.* (*13*). All these bacterial NIRs show 60% or higher sequence similarity. Two green NIRs from *Aci* (*14*) and *Afs* (*15*) and two blue ones from *Axn* (*16, 17*) and *Axg* (*18*) have quite similar trimer structures. A structural comparison of the Cu centers between green and blue NIRs reveals that the type 1 Cu site is flattened tetrahedral in green NIRs (*14, 15*) and distorted trigonal planar (*16, 17*) or distorted tetrahedral in blue NIRs (*18*). On the other hand, the type 2 Cu center bounded by a total of three His residues and a water molecule in a tetrahedral geometry is identical and superimposable among all NIRs. Figure 1 shows the type 2 Cu center of oxidized *Axg*NIR, where Asp98[4] and His255[4] conserved in the seven known NIR sequences are located at a key position. Aspartate-98 forms a hydrogen bond with a water ligand, which interacts with His255 through a hydrogen-bonding network *via* a bridging water molecule and replaced with nitrite. Strange *et al.* suggested a striking similarity in metal site geometry be-

[1] This work was supported by Grants-in-Aid for Scientific Research (Nos. 10129217, 11440198, and 11780428) from the Ministry of Education, Science, Sports and Culture of Japan, for which we express our thanks.

[2] To whom correspondence should be addressed. E-mail: kataoka@ch.wani.osaka-u.ac.jp

[3] The nucleotide sequence data coding for *Axg*NIR has been submitted to the DDBJ, EMBL, and GenBank nucleotide sequence databases with accession number AB013078.

[4] The residue numbers refer to the *Aci*NIR sequence.

Abbreviations: *Aci*, *Achromobacter cycloclastes* IAM 1013; *Afs*, *Alcaligenes faecalis* S-6; *Axg*, *Alcaligenes xylosoxidans* GIFU1051; *Axn*, *Alcaligenes xylosoxidans* NCIMB 11015; ESI, electrospray ionization; EXAFS, extended X-ray absorption fine structure; IPTG, isopropyl-1-thio-β-D-galactoside; MALDI-TOF, matrix assisted laser desorption/ionization-time of flight; MBP, maltose-binding protein; MES, 2-morpholinoethanesulfonic acid; NIR, nitrite reductase; *Rhs*, *Rhodobacter sphaeroides* 2.4.3; T2D, type 2 Cu-depleted.

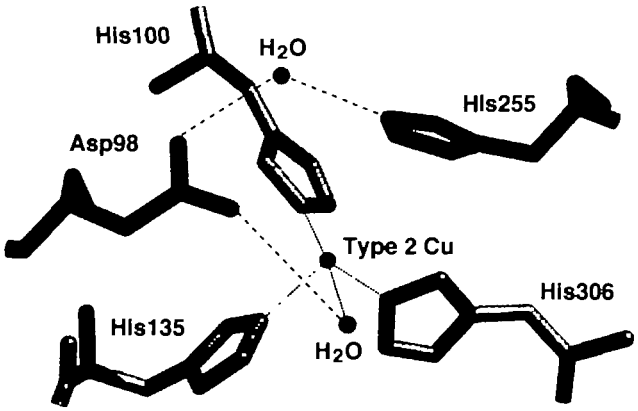

Fig. 1. **The type 2 Cu site of oxidized *Axg*NIR.** The residue numbers refer to the *Aci*NIR sequence.

tween the type 2 Cu site of NIR and the Zn site in carbonic anhydrase or thermolysin (*19*). Four Zn ligands in carbonic anhydrase (three His residues and a catalytic water molecule) and in thermolysin (two His, one Glu, and a water molecule) are superimposable onto those of NIR. Because the catalytically important residues of these Zn enzymes and Cu_2Zn_2 superoxide dismutase are located at positions structurally similar to Asp98 and His255 of NIR, it has been proposed that these two residues (Asp98 and His255) are important for catalysis (*19*, *20*). However, there is no direct evidence for their involvement in nitrite reduction.

To study the structure–function relationship of NIR, we report here the construction of an expression system of blue *Axg*NIR and the introduction of specific mutations at the conserved Asp98 and His255 positions.

MATERIALS AND METHODS

Materials—The vector pBluescript II and pMAL-c2X were purchased from STRATAGENE and New England Biolabs, respectively. *Taq* DNA polymerase, restriction endonucleases and other modifying enzymes were obtained from Takara Shuzo and Toyobo. *Taq* dye-terminator cycle sequencing kit (Applied Biosystems) was used for sequence determination. All other chemicals were of analytical grade.

Construction of Expression Plasmid—The gene encoding *Axg*NIR (*nirK*) was cloned and its complete DNA sequence was determined. (The DNA sequence has been submitted to the DDBJ, EMBL, and GenBank nucleotide sequence databases with the following accession number AB013078.) The plasmid pBAxNIR1 consists of a 2.4-kb fragment of *Axg* chromosomal DNA carrying *nirK* and a 2.9-kb plasmid pBluescript II fragment (unpublished).

A 1.2-kbp gene fragment consisting of the structural gene of NIR, *Sma*I linker, and *Bam*HI linker was amplified by PCR using two primers [P1: 5′-TTTACGATGGCCCCCGGGACCG-3′, coding for the N-terminal region of NIR and the *Sma*I digestion sequence (underline); P2: 5′-CATGGCGGGATCCTGGTCAGCG-3′ containing termination codon and the *Bam*HI digestion sequence (underline)] and cloned NIR gene (pBAxNIR1) as a template. The PCR products were digested with *Sma*I and *Bam*HI and cloned into expression plasmid pMAL-c2X digested with *Xmn*I and *Bam*HI to yield pMAxNIR3. The inserted gene was confirmed by DNA sequencing.

Expression and Purification of Recombinant NIR—*Escherichia coli* JM109 cells carrying pMAxNIR3 were grown in an LB medium supplemented with 50 μg/ml sodium ampicillin. After cultivation to a cell density of $O.D._{600\ nm}$ = 0.6 (about 3 h), 1 mM IPTG was added, and the bacteria were further incubated for 5 h at 37°C. The cells were harvested and disrupted by sonication. The cell extract was passed through an amylose resin column (New England Biolabs) equilibrated with 20 mM Tris-HCl buffer (pH 7.5) containing 0.1 M NaCl and 1 mM EDTA to bind the fused-recombinant protein containing maltose-binding protein (MBP). After washing the column, the fusion protein was eluted with the same buffer containing 10 mM maltose. The purified fusion protein was cleaved with factor Xa to release native apo-NIR, then the native apoenzyme was separated from MBP by passing through the amylose column again. The purified recombinant apo-enzyme was reconstituted with Cu by dialysis overnight at 4°C against 20 mM Tris-HCl buffer (pH 7.5) containing 1 mM $CuSO_4$. The type 2 Cu-depleted (T2D) NIR was prepared as described previously (*7*).

Mutagenesis—Site-directed mutagenesis was performed by a PCR method. For Asp98 mutants (D98A, D98N, and D98E), we employed two-step PCR (*21*) using sense and antisense oligonucleotide primers containing the same mutation. For His255 mutants (H255A, H255K, and H255R), we used antisense primers with an *Nco*I restriction site located 3′ downstream of the mutation site. The mutated DNA fragments were amplified using the above mutation primer, P1 or P2 primers, and pMAxNIR3 as a template, digested with an appropriate restriction enzyme, and exchanged with the wild-type fragment of pMAxNIR3. The mutant NIR genes were sequenced and expressed in *E. coli* JM109 as recombinant proteins.

Spectroscopy—Electronic absorption and CD spectra of recombinant and mutant NIRs were measured at room temperature with a Shimadzu UV-2200 and a JASCO J-500 spectropolarimeter equipped with a JASCO DP-501 data processor, respectively. EPR spectra of frozen protein samples were recorded at 77K with a JEOL JES-FE1X X-band spectrometer. The concentration of Cu was determined with a Nippon Jarrel Ash AA-880 Mark-II atomic absorption spectrophotometer.

Determination of NIR Activity—Nitrite reduction activity of native, recombinant, T2D, and mutant NIRs were determined by a steady-state method using benzyl viologen reduced with an excess of dithionite as an electron donor. The reaction mixture contained 0.1 M mixed buffer, 1.5 mM sodium nitrite, 2 mM dithionite, 1.25 mM benzyl viologen, and NIR in a total volume of 735 μl. For determination of kinetic parameters of NIR, the buffers were prepared by mixing 50 mM acetic acid, 50 mM MES, and 100 mM Tris, and titrating to the desired pH values with HCl or NaOH. The ionic strengths of the mixed buffers were maintained at 0.1 by the addition of NaCl according to Ellis and Morrison (*22*). To exclude oxygen, all procedures were carried out in argon atmosphere. In a 1.5-ml microtube, an appropriate amount of nitrite, dithionite, and benzyl viologen were dissolved in 1 ml of the buffer sparged with high-purity argon gas over 5 min. A 700-μl portion of this solution was transferred into an argon-exchanged cuvette (2 mm light-path length), which was closed immediately with a rubber cap.

The reaction was started by the injection of NIR (35 μl) through the rubber cap. The oxidation rate of reduced benzyl viologen was monitored spectrophotometrically at 550 nm [ε = 10.4 mM^{-1} cm^{-1} (*23*)] at 25°C.

Nitrite consumption was also determined by the diazotization method (*24*). In this case, the reaction was carried out in the reaction vessel with 3 ml of the same mixture under argon gas atmosphere at 25°C. Aliquots of 100 μl were withdrawn at various times, and the reaction was terminated by vigorous mixing with air to decompose dithionite and reduced benzyl viologen prior to the colorimetric measurement.

RESULTS AND DISCUSSION

Expression and Purification of Recombinant NIR—We have cloned and sequenced the NIR gene from *A. xylosoxidans* GIFU1051. Recently, the NIR gene from *A. xylosoxidans* NCIMB11015 (*Axn*) has been reported by two groups (*12*, *13*). The open reading frames of *Axg*NIR and *Axn*NIR differed by only 1 base in a total gene sequence of 1,083 bp, and the protein sequences of *Axg*NIR and *Axn*NIR were identical (360 amino acids, data not shown). Since there is no information available about the N-terminal amino acid sequence of *Axg*NIR, the molecular mass of apo-NIR was determined by ESI and MALDI-TOF mass spectroscopies. A mass spectral value of M_r = 36,540 suggest that Gln25 is the N-terminus (calculated M_r = 36,523) and that this is preceded by the signal peptide of 24 residues. This result completely agreed with the protein sequence of *Axn*NIR reported by Vandenberghe *et al.* (*25*), indicating that these two NIRs are identical to each other.

For the expression of *Axg*NIR, we used the protein fusion expression system (New England Biolabs). First, we inserted the gene coding for mature *Axg*NIR into *Xmn*I site of pMAL-c2X. The resulting plasmid (pMAxNIR1) could express the fusion protein in which the N-terminus Gln residue is connected directly after the protease factor Xa recognition sequence. However, this MBP-fusion NIR was not digested by factor Xa, because of the negative charges of the Asp2 and Asp4 residues close to the recognition sequence. Therefore, we constructed the expression plasmid pMAxNIR3, which has the gene coding for the mature protein and the partial signal sequence of *Axg*NIR (5 amino acid residues). With pMAxNIR3, a large amount of the recombinant enzyme was expressed in *E. coli* as a fusion protein with MBP. The expressed MBP-fusion protein was easily purified with an amylose resin column and the MBP-domain was removed by digestion with factor Xa to release recombinant apo-*Axg*NIR (Fig. 2). Approximately 10 mg of the recombinant protein was obtained from 4 g of wet cells (1 liter culture medium).

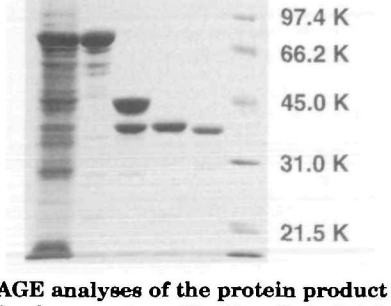

Fig. 2. **SDS-PAGE analyses of the protein product during expression and subsequent purification**. Lane 1, total cell lysate of *E. coli* JM109 harboring pMAxNIR3; lane 2, amylose column purified MBP-fusion protein; lane 3, purified MBP-fusion protein after factor Xa cleavage; lane 4, purified recombinant *Axg*NIR; lane 5, native *Axg*NIR; lane 6, standard proteins (Bio-Rad, LMW).

The N-terminal sequence of the recombinant protein was determined to be Gly-Thr-Ala-Trp-Ala-Gln-Asp-Ala, which corresponds to the genetically designed sequence. The quaternary structure of the recombinant protein was compared to those of the native enzyme by gel-filtration chromatography. The two proteins eluted at almost identical volumes on TSK gel $SW3000_{XL}$ column (data not shown). Therefore, the recombinant protein with an extension of 5 amino acid residues has a trimer structure like native *Axg*NIR.

Characterization of Recombinant NIR—The oxidized type 1 Cu sites in two blue *Alcaligenes* NIRs exhibit *ca.* 590-nm absorption bands and EPR signals with an axial symmetry (*7*). The electronic absorption spectra of native and recombinant oxidized *Axg*NIRs in Fig. 3A are indistinguishable and display one intense band at 593 nm and two broad bands at 470 and 775 nm assigned to S(Cys)-Cu(II) charge transfer transitions of type 1 Cu. The ratio of $\varepsilon_{470\ nm}/\varepsilon_{593\ nm}$ (4.7) and the absorption coefficient at 593 nm (ε =

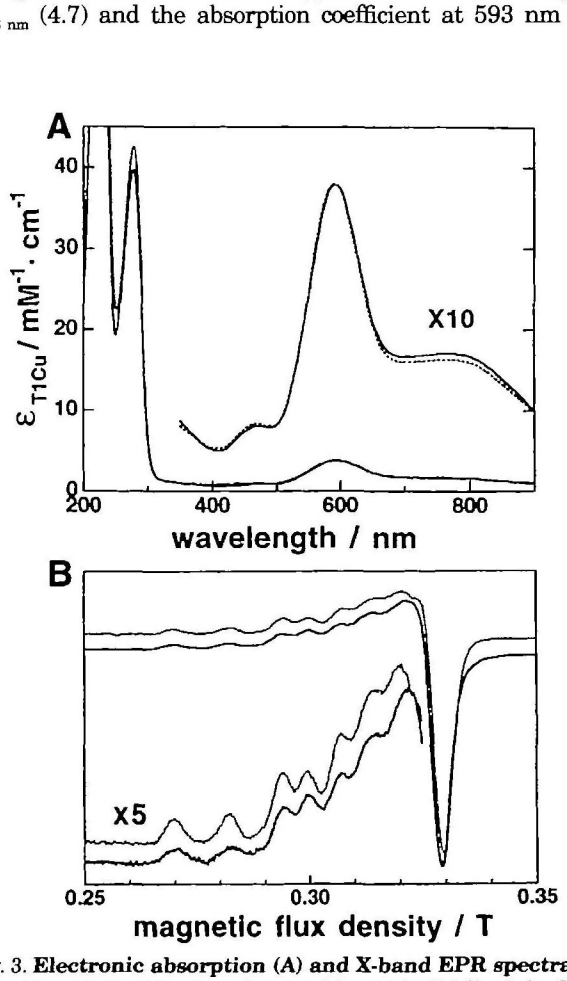

Fig. 3. **Electronic absorption (A) and X-band EPR spectra (B) of native (dotted line) and recombinant (solid line) *Axg*NIR.** Conditions: (A) 0.1 M potassium phosphate buffer (pH 7.0) at room temperature; (B) 0.1 M Tris-HCl buffer (pH 7.5) at 77 K.

3,800 $M^{-1} cm^{-1}$) are identical in the native and the recombinant forms. The visible CD spectrum of the recombinant displays a positive extremum at 400 nm and two troughs at 470 and 670 nm, like the native protein (data not shown).

Figure 3B shows the 77K EPR spectra of native and recombinant *Ax*gNIRs. The EPR signal of the recombinant displays the parameters of $g_{//} = 2.21$, $g_{\perp} = 2.06$, and $A_{//} = 6.7$ mT for the type 1 Cu and $g_{//} = 2.31$ and $A_{//} = 11.7$ mT for the type 2 Cu. These values are comparable to those of the native protein (*7*), indicating that the coordination structures of the type 1 and 2 Cu sites in the recombinant are the same as those in the native enzyme. All these characteristic spectroscopic properties of *Ax*gNIR are retained in the recombinant protein, implying that the 5 amino acid residues added in the N-terminal do not affect the coordination structure of the Cu sites. The copper content of the recombinant protein was measured by atomic absorption spectroscopy. The ratio of type 1 Cu : type 2 Cu is 1 : 0.9 per subunit.

Steady-State Kinetics of Recombinant NIR—The nitrite reduction activities of native and recombinant *Ax*gNIRs were determined by the steady-state method using dithionite/benzyl viologen as an electron donor. The apparent catalytic rate constants (k_{app}) for the native and recombinant proteins were respectively 1,640 ± 80 and 1,670 ± 92 s^{-1} at their optimum pH (pH 5.5), being comparable to *Ax*nNIR activity using dithionite/methyl viologen as an electron donor (*26*). The enzyme activities were also determined by colorimetric assay of NO_2^- (*7*). In this stopped-time assay, we changed the electron donor from TMPD in our previous method to dithionite/benzyl viologen. The pseudo first-order rate constant (1,230 ± 110 s^{-1} at pH 5.5) of the recombinant by the present method was similar to the above apparent k_{app} value. This value is larger than that by our previous method [12 s^{-1} (*7*)] by a factor of 100, suggesting that benzyl viologen can donate an electron to NIR more effectively than TMPD. The apo-NIR showed no detectable activity with dithionite/benzyl viologen in either the steady-state or the colorimetric assay system.

Since the rate of direct nitrite reduction with benzyl viologen (background) is fast at low pH, the apparent K_m for nitrite was determined at pH 7.0 where no background is observed. The apparent K_m values for NO_2^- of native and recombinant *Ax*gNIR's were estimated to be 37 and 23 μM, respectively, in good agreement with the value of *Ax*nNIR [34 μM at pH 7.5 (*26*)].

Properties of Mutant and T2D NIRs—To elucidate the catalytic residue(s) of NIR, two nonligating polar residues (Asp98 and His255) located near the type 2 Cu site were substituted. Asp98, whose β-carboxylate oxygen is hydrogen-bonded to the water ligand, was changed to Ala, Asn, or Glu. His255, which interacts with Asp98 through a hydrogen-bonding network, was changed to Ala, Lys, or Arg. All the mutant NIRs were expressed and purified by the same procedures as the recombinant enzyme.

The type 2 Cu/type 1 Cu ratio of Cu-reconstituted mutant NIRs was estimated to be in the range of 0.7–1.0. The electronic absorption and CD spectra of all the mutants were essentially identical to the spectra of recombinant *Ax*gNIR (data not shown). On the other hand, EPR spectra of the His255 mutants were changed, as observed in the mutant *Rhs*NIR in which the corresponding His residue was replaced with Glu [H287E (*10*)]. The type 2 Cu spectral features of the mutants remained but were broadened. These findings indicate that the local conformation of the type 1 Cu site does not change, but that of the type 2 Cu site is slightly influenced by the replacement of His around type 2 Cu.

Steady-state kinetic analyses were performed with the purified mutant enzymes to elucidate the functional roles of Asp98 and His255 (Table I). The k_{app} values of all the Asp98 mutants decrease by 1.7–2.8% compared with those of the recombinant enzyme at pH 7.0. Furthermore, the apparent K_m values for nitrite of the Asp98 mutants are greatly increased in D98A (K_m = 1,500 μM) and D98N (K_m = 4,600 μM). However, D98E, which carries the same negative charge as Asp, shows only a small increase in the K_m value. The fact that the Asp98 mutants have the large K_m values for NO_2^- demonstrates that the negative charge of Asp98 is indispensable to anchor NO_2^-, as shown by the X-ray structure analysis (*14*). The catalytic efficiencies (k_{app}/K_m) of D98A and D98N are dramatically decreased by a factor of 1/1,000 compared to that of the recombinant. These results suggest that Asp98 is important not only for NO_2^- anchoring to the active site but also for proton donation.

In the case of the three His255 mutants, the k_{app} values are markedly decreased, being only 0.4% of that of the recombinant at pH 7.0 (Table I). A similar decrease in catalytic activity was also observed in H287E of *Rhs*NIR [0.3%

TABLE I. **Kinetic constants of recombinant, native, T2D, and mutant NIRs (pH 7.0).**

NIRs	k_{app} (s^{-1})	K_m (μM)	k_{app}/K_m ($\mu M^{-1} s^{-1}$)
recombinant	470 ± 20	23 ± 8	20
native	380 ± 10	37 ± 2	10
T2D	46 ± 5	34 ± 12	1.3
D98A	10 ± 0.3	1,500 ± 90	0.0067
D98N	8.0 ± 0.1	4,600 ± 100	0.0017
D98E	13 ± 0.4	390 ± 57	0.033
H255A	1.7 ± 0.1	520 ± 56	0.0032
H255K	1.6 ± 0.2	120 ± 29	0.013
H255R	1.5 ± 0.1	45 ± 11	0.033

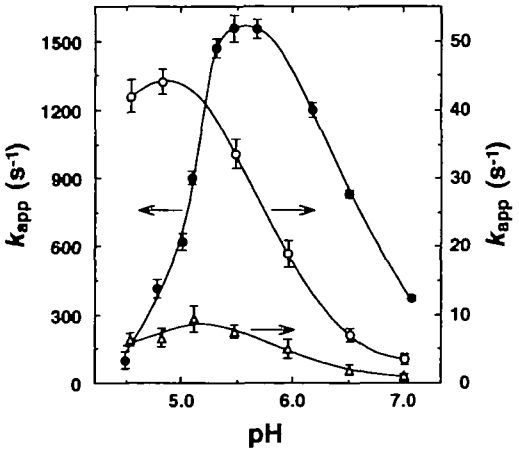

Fig. 4 **Effect of pH on the reaction rates of native, Asp98Ala, and His255Ala NIRs.** Filled circles, native NIR (left ordinate); open circles, Asp98Ala mutant (right ordinate); open triangles, His255Ala mutant (right ordinate). The apparent catalytic rate constants were determined with the nitrite concentration of 1.5 mM.

of the wild type at pH 6.2 (*10*)]. The K_m values for nitrite of H255A and H255K are considerably larger than that of the recombinant enzyme, whereas the value of H255R is similar to that of the recombinant. The K_m value was not changed in H287E of *Rhs*NIR (*10*). The comparable K_m values of H255R and the native enzyme indicate that His255 is not directly involved in nitrite binding but would control the position of Asp98 through a hydrogen-bonding network.

The pH-dependence of the reaction rates of D98A and H255A was compared with that of the native enzyme using mixed-buffer system described in "MATERIALS AND METHODS" (Fig. 4). The pH-profile for the native enzyme is bell-shaped with the optimum near pH 5.5 and is substantially same as that of *Axn*NIR (*26*). This curve indicates the presence of two proton dissociation residues with pK_a values of about 5 and 7. The pulse radiolysis study of *Aci* and *Axg*NIRs also revealed the existence of proton dissociation groups having pK_a values of 5.0 and 7.0 (*27*). The optimum pH values of both D98A and H255A are shifted to acidic pH. The major effect of the mutation on the protonation of the residue with a pK_a of 7 (probably His255) suggests that the mutated residues do not form a hydrogen-bonding network. Therefore, from the above kinetic data, we concluded that Asp98 and His255 must play an important role in the catalytic process and would give pK_a values of 5.0 and 7.0, respectively.

T2D-*Axg*NIR retains 25% of the original activity and, interestingly, the apparent K_m for nitrite hardly changes from that of the native enzyme (34 μM, Table I). The binding of NO_2^- to T2D-*Axn*NIR was observed by the column equilibration method (*26*). Since NO_2^- does not interact with the type 1 Cu center of T2D-*Axn*NIR (*19*), NO_2^- will bind to the type 2 Cu site without Cu in the T2D enzyme. The almost equal K_m values of the native and T2D forms indicate that the nitrite-binding process is not controlled by type 2 Cu but by the local environment of the active site. The hydrogen-bonding network around type 2 Cu of *Aci*NIR is very stable even when type 2 Cu is depleted (*14*). In the active site of T2D-*Aci*NIR, the water molecule (so called T2D water) was observed at the position between the water ligand and type 2 Cu in the holo-enzyme, and was anchored by His100, His135, and Asp98 (*14*). The substrate is probably replaced by this T2D water, of which a proton will be abstracted by Asp98, and then reduced, as proposed in the native enzyme (vide infra).

Reaction Mechanism of NIR—From the crystallographic structures of nitrite-soaked *Aci*NIR and *Axn*NIR, NO_2^- is ligated to type 2 Cu in an asymmetric bidentate manner with two oxygen atoms (*8*, *14*). The nitrite molecule is oriented by hydrogen-bonding between one of two oxygen atoms of nitrite and β-carboxylate of Asp98. On the basis of the present kinetic results together with the active site structure of NIR, we propose the reaction mechanism of NIR depicted in Fig. 5. In the first step, the substrate, NO_2^- displaces the water ligand, which leaves a proton on Asp98 and is released as OH^- (*14*). The protonated β-carboxylate group of Asp98 is hydrogen-bonded with the oxygen atom of NO_2^- bound to type 2 Cu (step 1). Type 2 Cu accepts one electron from type 1 Cu, and the proton is transferred to NO_2^- to form NOOH intermediate (step 2). In the crystal structure of oxidized *Axg*NIR, the side-chain of His255 has temperature factors (B-factors) considerably lowered by

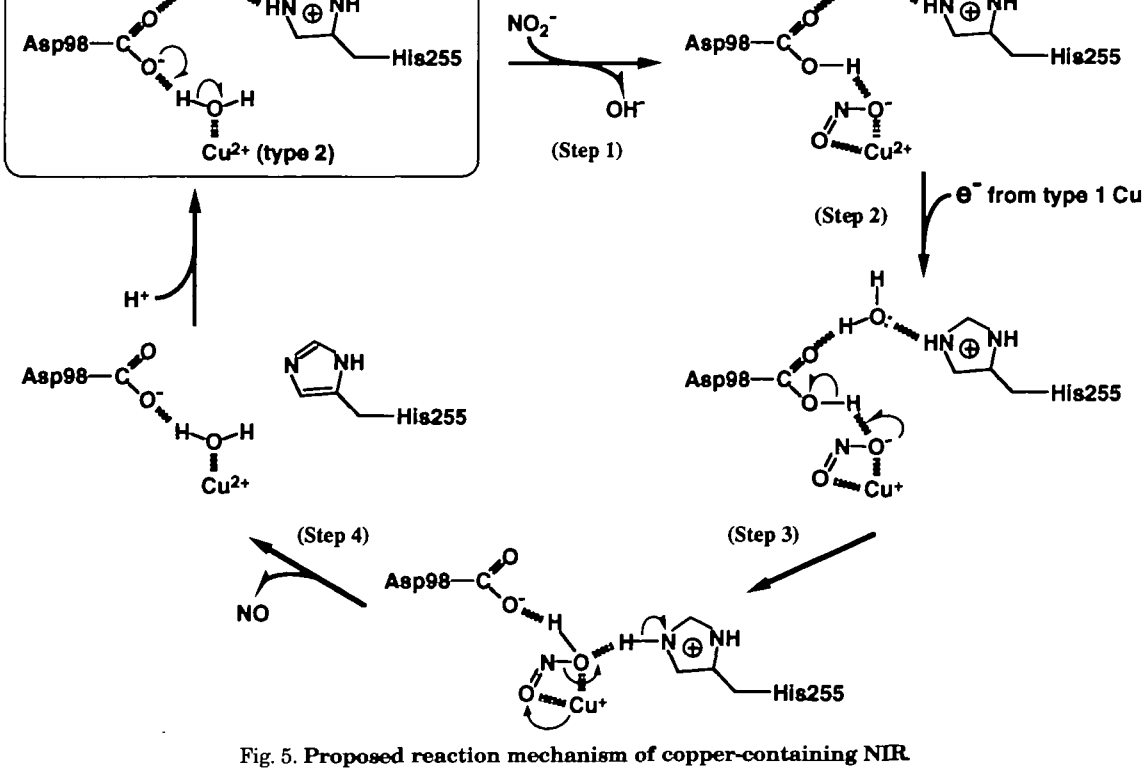

Fig. 5. **Proposed reaction mechanism of copper-containing NIR.**

hydrogen-bonding to the water molecule bridging to Asp98. On the contrary, the B-factors of those of reduced *Axg*NIR are increased more than the average B-factor of all side-chains in the protein (unpublished data). This result indicates that the hydrogen-bonding network of Asp98-water-His255 will be broken in the reduced state. Moreover, there is a space through which the side-chain of His255 can approach the intermediate. As shown in the pH profile of native *Axg*NIR (Fig. 4), His255 is probably protonated at optimum pH. The movement of protonated His255 toward NOOH and the electron transfer from type 2 Cu (I) to NOOH may facilitate cleavage of the N-O bond (step 3). Another proton will be donated from the imidazolium group of His255 to form a water molecule coordinated to type 2 Cu, and NO is simultaneously generated (step 4). Consequently, Asp98 and His255 work as general acid-base catalysts which provide the two protons required for nitrite reduction (proton shuttling residues). This general acid-base function of the conserved Asp98 and His255 residues is probably common in the Cu-NIR family.

We also thank Prof. Katsuyuki Tanizawa and Dr. Ryuichi Matsuzaki, the Institute of Scientific and Industrial Research, Osaka University, for the sequence analyses, and Prof. Ryuichi Arakawa and Dr. Tsuyoshi Fukuo, Faculty of Engineering, Kansai University, for the measurements of ESI and MALDI-TOF mass spectra. We also grateful to Dr. Tsuyoshi Inoue and Prof. Yasushi Kai, Graduate School of Engineering, Osaka University, for the X-ray crystal structure analysis of NIR.

REFERENCES

1. Zumft, W.G. (1992) *The Prokaryotes* (Balows, A. *et al.*, eds.) Vol. 1, pp. 554–582, Springer, Berlin, Heidelberg, New York
2. Zumft, W.G. (1997) Cell biology and molecular basis of denitrification. *Microbiol. Mol. Biol. Rev.* **61**, 533–616
3. Averill, B.A. (1996) Dissimilatory nitrite and nitric oxide reductases. *Chem. Rev.* **96**, 2951–2964
4. Masuko, M., Iwasaki, H., Sakurai, S., Suzuki, S., and Nakahara, A. (1984) Characterization of nitrite reductase from a denitrifier, *Alcaligenes* sp. NCIB 11015. A novel copper protein. *J. Biochem.* **96**, 447–454
5. Iwasaki, H. and Matsubara, T. (1972) A nitrite reductase from *Achromobacter cycloclastes*. *J. Biochem.* **71**, 645–652
6. Kakutani, T., Watanabe, H., Arima, K., and Beppu, T. (1981) Purification and properties of a copper-containing nitrite reductase from a denitrifying bacterium, *Alcaligenes faecalis* Strain S-6. *J. Biochem.* **89**, 453–461
7. Suzuki, S., Deligeer, Yamaguchi, K., Kataoka, K., Kobayashi, K., Tagawa, S., Kohzuma, T., Shidara, S., and Iwasaki, H. (1997) Spectroscopic characterization and intermolecular electron transfer processes of native and type 2 Cu-depleted nitrite reductases. *J. Biol. Inorg. Chem.* **2**, 265–274
8. Chen, J.-Y., Chang, W.-C., Chang, T., Chang, W.-C., Liu, M.-Y., Payne, W.J., and LeGall, J. (1996) Cloning, characterization, and expression of the nitric oxide-generating nitrite reductase and the blue copper protein genes of *Achromobacter cycloclastes*. *Biochem. Biophys. Res. Commun.* **219**, 423–428
9. Nishiyama, M., Suzuki, J., Kukimoto, M., Ohnuki, T., Horinouchi, S., and Beppu, T. (1993) Cloning and characterization of a nitrite reductase gene from *Alcaligenes faecalis* and its expression in *Escherichia coli*. *J. Gen. Microbiol.* **139**, 725–733
10. Olesen, K., Veselov, A., Zhao, Y., Wang, Y., Danner, B., Scholes, C.P., and Shapleigh, J.P. (1998) Spectroscopic, kinetic, and electrochemical characterization of heterologously expressed wild-type and mutant forms of copper-containing nitrite reductase from *Rhodobacter sphaeroides 2.4.3*. *Biochemistry* **37**, 6086–6094
11. Yabuuchi, E., Yano, I., Goto, S., Tanimira, E., Ito, T., and Ohyama, A. (1974) Description of *Achromobacter xylosoxidans* Yabuuchi and Ohyama 1971. *Int. J. Syst. Bacteriol.* **24**, 470–477
12. Suzuki, E., Horikoshi, N., and Kohzuma, T. (1999) Cloning, sequencing, and transcriptional studies of the gene encoding copper-containing nitrite reductase from *Alcaligenes xylosoxidans* NCIMB 11015. *Biochem. Biophys. Res. Commun.* **255**, 427–431
13. Prudêncio, M., Eady, R.R., and Sawers, G. (1999) The blue copper-containing nitrite reductase from *Alcaligenes xylosoxidans*: Cloning of the *nir*A gene and characterization of the recombinant enzyme. *J. Bacteriol.* **181**, 2323–2329
14. Adman, E.T., Godden, J.W., and Turley, S. (1995) The structure of copper-nitrite reductase from *Achromobacter cycloclastes* at five pH values, with NO_2^- bound and with type II copper depleted. *J. Biol. Chem.* **270**, 27458–27474
15. Murphy, M.E.P., Turley, S., and Adman, E.T. (1997) Structure of nitrite bound to copper-containing nitrite reductase from *Alcaligenes faecalis*. mechanistic implications. *J. Biol. Chem.* **272**, 28455–28460
16. Dodd, F.E., Hasnain, S.S., Abraham, Z.H.L., Eady, R.R., and Smith, B.E. (1997) Structures of a blue-copper nitrite reductase and its substrate-bound complex. *Acta Cryst.* **D53**, 406–418
17. Dodd, F.E., Van Beeumen, J., Eady, R.R., and Hasnain, S.S. (1998) X-ray structure of a blue-copper nitrite reductase in two crystal forms. The nature of the copper sites, mode of substrate binding and recognition by redox partner. *J. Mol. Biol.* **282**, 369–382
18. Inoue, T., Gotowda, M., Deligeer, Kataoka, K., Yamaguchi, K., Suzuki, S., Watanabe, H., Gohow, M., and Kai, Y. (1998) Type 1 Cu structure of blue nitrite reductase from *Alcaligenes xylosoxidans* GIFU 1051 at 2.05 Å resolution: Comparison of blue and green nitrite reductases. *J. Biochem.* **124**, 876–879
19. Strange, R.W., Dodd, F.E., Abraham, Z.H.L., Grossmann, J.G., Brüser, T., Eady R.R., Smith, B.E., and Hasnain, S.S. (1995) The substrate-binding site in Cu nitrite reductase and its similarity to Zn carbonic anhydrase. *Nat. Struct. Biol.* **2**, 287–292
20. Strange, R.W., Murphy, L.M., Dodd, F.E., Abraham, Z.H.L., Eady, R.R., Smith, B.E., and Hasnain, S.S. (1999) Structural and kinetic evidence for an ordered mechanism of copper nitrite reductase. *J. Mol. Biol.* **287**, 1001–1009
21. Higuchi, R. (1989) in *PCR Technology* (Erlich, H.A., ed.) pp. 61–88, Stockton Press, New York
22. Ellis, K.J. and Morrison, J.F. (1982) Buffers of constant ionic strength for studying pH-dependent processes. *Methods Enzymol.* **87**, 405–426
23. Michalski, W.P., Hein, D.H., and Nicholas, D.J. (1986) Purification and characterization of nitrous oxide reductase from *Rhodopseudomonas sphaeroides* f.sp. *denitrificans*. *Biochim. Biophys. Acta* **872**, 50–60
24. Masuko, M. and Iwasaki, H. (1984) Activation of nitrite reductase in a cell-free system from the dinitrifier *Alcaligenes* sp. by freeze-thawing. *Plant Cell Physiol.* **25**, 439–446
25. Vandenberghe, I.H.M., Meyer, T.E., Cusanovich, M.A., and Van Beeumen, J.J. (1998) The covalent structure of the blue copper-containing nitrite reductase from *Achromobacter xylosoxidans*. *Biochem. Biophys. Res. Commun.* **247**, 734–740
26. Abraham, Z.H.L., Smith, B.E., Howes, B.D., Lowe, D.J., and Eady, R.R. (1997) pH-dependance for binding a single nitrite ion to each type-2 copper center in the copper-containing nitrite reductase of *Alcaligenes xylosoxidans*. *Biochem. J.* **324**, 511–516
27. Kobayashi, K., Tagawa, S., Deligeer, and Suzuki, S. (1999) The pH-dependent changes of intermolecular electron transfer on copper-containing nitrite reductase. *J. Biochem.* **126**, 408–412